Available online at www.sciencedirect.com
ScienceDirect
Engineering Fracture Mechanics 75 (2008) 341–354
Engineering Fracture Mechanics
www.elsevier.com/locate/engfracmech

Optimising FSW process parameters to minimise defects and maximise fatigue life in 5083-H321 aluminium alloy

H. Lombard [a,b], D.G. Hattingh [b], A. Steuwer [a,c], M.N. James [a,*]

[a] School of Engineering, University of Plymouth, Plymouth, PL4 8AA England, United Kingdom
[b] ATCS, Nelson Mandela Metropolitan University, Port Elizabeth, South Africa
[c] FaME38, ILL-ESRF, 6 Rue J. Horowitz, BP 156, 38042 Grenoble, Cedex 9, France

Received 3 December 2006; received in revised form 23 January 2007; accepted 28 January 2007
Available online 9 February 2007

Abstract

This paper presents a systematic approach to optimising FSW process parameters (tool rotational speed and feed rate) through consideration of frictional power input. Frictional power governs the tensile strength and the fatigue life in this 5083-H321 alloy through its effect on plastic flow processes in the thermo-mechanically affected zone (TMAZ) of the weld. Although, a close relationship therefore exists between tensile strength and fatigue performance, this arises from their joint dependence on the occurrence of certain defect types that are apparently specific to certain strain hardened aluminium alloys that are FS welded. These defects are related to plastic flow processes and have a strong influence on crack paths in FS welded 5083-H321 alloy. Weld residual stresses have been extensively measured using synchrotron X-ray diffraction strain scanning and are governed by heat input into the weld. There is no clear relationship between peak values of residual stresses and fatigue performance. The work indicates that rotational speed is the key parameter governing tool torque, temperature, frictional power and hence tensile strength and fatigue performance.

Keywords: Friction stir welding; Process optimisation; Tool speed; Tool feed; Tool pitch; Energy input; Fatigue life; Weld defects

1. Introduction

Friction stir welding (FSW) is a relatively new solid state joining process that offers the potential for joints with high fatigue strength, low preparation and little post-weld dressing. Other benefits include generally low defect populations (compared with fusion welding) and the ability to join dissimilar metals. The technique has hence attracted significant interest from the aerospace and transportation industries and an extensive literature exists on FSW (see, for instance, the comprehensive review given in Ref. [1]). To date, however, there are few reported systematic studies of process optimisation in terms of the linkages among process parameters (primarily tool rotational speed and feed rate, and the forces on the tool), defect population, residual stresses,

* Corresponding author.
E-mail address: mjames@plymouth.ac.uk (M.N. James).

0013-7944/$ - see front matter © 2007 Elsevier Ltd. All rights reserved.
doi:10.1016/j.engfracmech.2007.01.026

mechanical properties and fatigue performance [2–5]. In particular the use of instrumented tools that can provide data on heat, power and energy input into the welds is in its infancy [6]. Thus welding parameters (tool speed and feed, tool geometry, downwards tool force) are usually established empirically for individual cases. It would be clearly advantageous to be able to reduce this empiricism and to be able to identify optimum process parameter combinations and optimum tool geometries in relation to mechanical properties and dynamic performance of FS welds.

This paper builds on previously published work [6] that reported the potential use of data that could be obtained from an instrumented tool post (torque, temperature, forces on the tool). It considers a structural strain hardened aluminium alloy, 5083-H321, which has been previously reported [7] to show unusual pseudo-bond defects in FS welds. The work reported here has demonstrated that clear linkages do exist between fatigue performance, crack paths, defect type and process parameters. The influence of basic process parameters (tool rotational speed and feed rate) can be characterised through frictional power and heat input calculations. These, in turn, reflect the plastic flow processes that occur in the TMAZ and which lead to forces experienced by the tool. Data reported in this paper can be linked and interpreted to provide a predictive capability for structure-process-property relationships in FSW. The basic hypothesis underlying the work is schematically illustrated in Fig. 1. Fig. 2 illustrates the FSW process and defines coordinate directions used for the forces on the tool, plus the advancing and retreating sides of the weld. As a result of the combination of tool rotation and forwards movement during welding, the material properties and residual stresses in the weld are slightly different on the advancing and retreating sides of the weld.

Fig. 1 indicates that the independent process input parameters of tool rotational speed, feed rate and tool shoulder plunge depth, interact with joint geometry and alloy to give rise to other dependent process parameters such as tool temperature rise, downwards forging force on the tool shoulder, tool torque and tool forces. These vary along the weld but attain peak values after about 100 mm of welding, as shown in Fig. 3. Torque, tool temperature and the in-plane forces (F_X and F_Y) then show quasi-static behaviour with a slight decay occurring in peak values over the next 500 mm of welding. In contrast, the downwards forging force (F_Z) steadily decreases by around 30% as welding continues before increasing again towards the end of the weld. In terms of fundamental understanding of FSW processes it would be preferable to control the welding forces in the three coordinate directions. The development of advanced FSW machines for research purposes, such

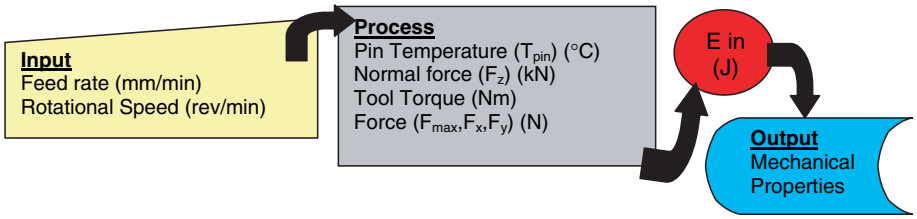

Fig. 1. Schematic illustration of proposed linkages between input and output parameters in FSW.

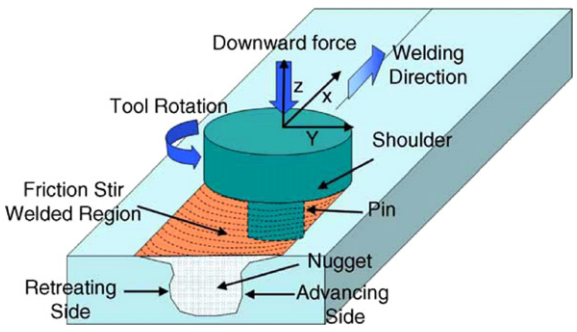

Fig. 2. Illustration of FSW process [3].

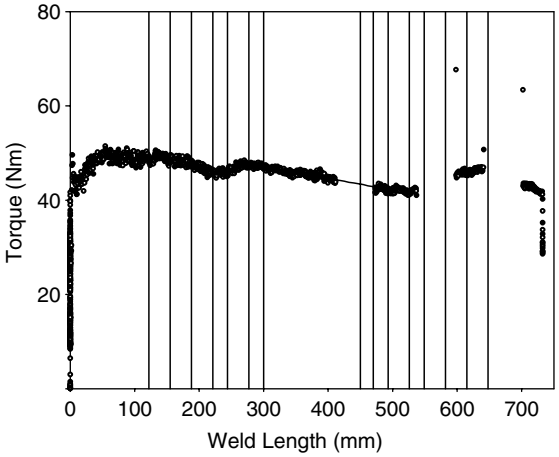

Fig. 3a. Variation of tool torque with welding distance. Welds were 750 mm long.

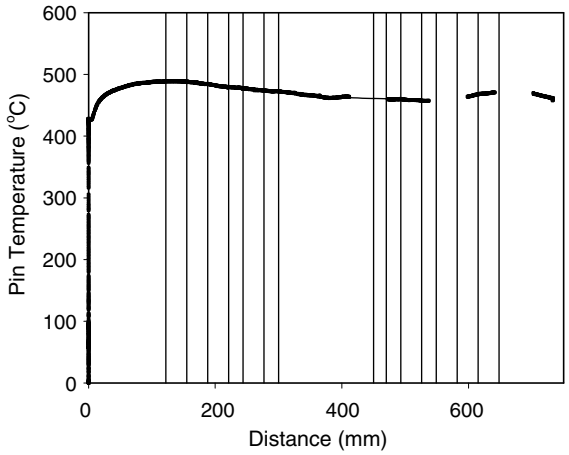

Fig. 3b. Variation of tool pin temperature with welding distance. Welds were 750 mm long.

as the MTS ISTIR Process Development System, allows this possibility and such a machine will be installed at the Nelson Mandela Metropolitan University during 2007. Irrespective of whether the downwards forging force is controlled or not, data reported in this paper demonstrate that tool-material interactions can be characterised by energy input to the weld (heat input or frictional power) and related to weld characteristics like residual stresses, mechanical properties and fatigue performance.

Thus the purpose of this paper is to develop the framework for a predictive methodology for the performance under static and dynamic loading of FS welds in 5083-H321 aluminium alloy, using input weld parameters of tool speed and feed rate. It will be seen that frictional power governs the tensile strength and the fatigue life in this alloy through its effect on plastic flow processes in the thermo-mechanically affected zone (TMAZ) of the weld. Although, a close relationship therefore exists between tensile strength and fatigue performance, this arises from their linked dependence on the occurrence of certain defect types that are apparently specific to strain hardened aluminium alloys that are FS welded. These defects are related to plastic flow processes and have a strong influence on crack paths in FS welded 5083-H321 alloy.

2. Experimental details and process conditions

This work used 6 mm plates, 100 mm wide, joined by welds 750 mm long. Tensile and fatigue specimens were cut from the same positions towards the middle section of each weld where process parameters such

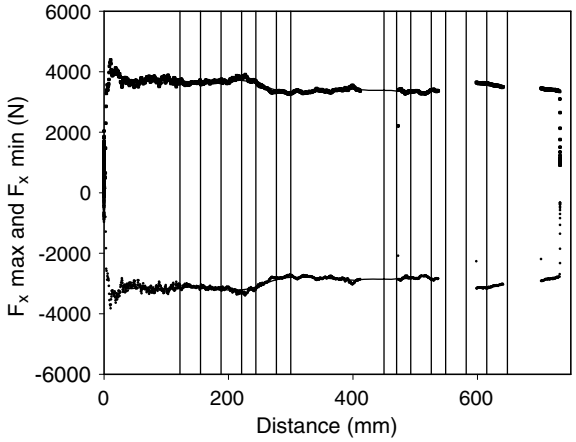

Fig. 3c. Variation of in-plane force F_X with welding distance. Welds were 750 mm long.

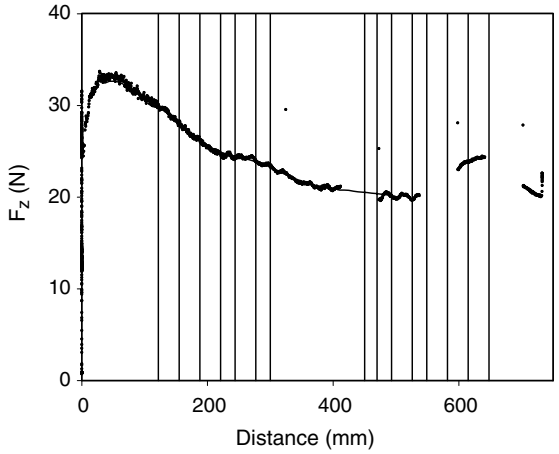

Fig. 3d. Variation of downwards forging force with welding distance. Welds were 750 mm long.

as tool temperature, torque, and forces attain quasi-static values. The FS welding tool had a shoulder radius of 25 mm while the fluted and threaded pin was 10 mm in diameter and 5.7 mm long (see Fig. 4). The forging action of the tool shoulder was enhanced via a forwards tool tilt angle of 2.5°. Table 1 gives the combinations of tool rotational speed and feed values chosen for this research. Tool speed and feed can be combined into a single characterising parameter giving tool pitch per revolution, and the test matrix has been selected to provide several combinations of tool speed and feed rate corresponding to a series of pitch values between 0.2 and 0.5 mm/min. An attempt was made to select feed rates with an approximate ratio of 1:1.5:2 and to select similar rotational speeds at each pitch value (around 300, 400 and 600 rpm). One aim of this work was to determine which input parameter would provide the best correlating parameter for weld performance. The work indicates that rotational speed is the key parameter governing tool torque, temperature, frictional power and hence tensile strength and fatigue performance.

Table 2 gives the average measured values of parent plate and weld tensile properties. These data were obtained from tensile specimens (12.5 mm across the gauge section) which were left in either the as-rolled or as-welded form, i.e. they were not machined on the plate surfaces. Weld data is given as the average of three sets of specimens cut from three positions in the quasi-static region of the weld run (Fig. 3). The ratios of weld tensile and proof strength to parent plate data are very similar to those reported by Peel [8] for FS welds in this 5083-H321 alloy and hence represent 'typical' rather than 'poorly' made welds. Weld strength ratios are low compared with those reported for other aluminium alloys, and this can be linked to the presence of particular

Fig. 4. Flute tool geometry used to make the FS welds.

Table 1
Tool rotational speed, feed and pitch values used in this work

85 mm/min			135 mm/min			185 mm/min		
RPM[a]	Pitch[b] (mm/rev)	Weld no.[c]	RPM	Pitch (mm/rev)	Weld no.	RPM	Pitch (mm/rev)	Weld no.
400	0.21	8	635	0.21	11	870	0.21	4
266	0.32	6	423	0.32	2	617	0.3	10
201	0.42	3	318	0.42	9	436	0.42	1
			254	0.51	5	348	0.53	7

[a] RPM, tool rotational speed in revolutions per minute.
[b] Pitch, distance moved forwards along the weld by the tool during one revolution.
[c] Weld no., identification number of a particular specimen.

Table 2
Tensile (UTS) and 0.2% proof strength data for 5083-H321 parent plate and the FS welds

Weld No.	Average UTS[a] (MPa)	UTS/PP[b]	Average 0.2% Proof Strength[c] (MPa)	Proof/PP[d]
1	289	0.78	171	0.67
2	241	0.65	153	0.60
3	313	0.84	161	0.63
4	254	0.68	144	0.57
5	308	0.83	165	0.65
6	315	0.85	164	0.65
7	294	0.79	150	0.59
8	308	0.83	145	0.57
9	273	0.74	145	0.57
10	310	0.84	148	0.58
11	306	0.82	141	0.56
Parent plate	371		254	

[a] Average UTS value across the weld obtained from 3 tests in each welded plate.
[b] UTS/PP = ratio of average tensile strength of welded specimen to the parent plate value (average of 3 tests).
[c] Average 0.2% proof strength value from 3 tests in each welded plate.
[d] Proof/PP = ratio of average 0.2% proof strength for each welded plate to the parent plate value (average) for the 0.2% proof strength.

quasi-bond defects that occur in this condition of the 5083 alloy [7]. It would therefore be anticipated that activation of such defects would be a dominant feature in the static and dynamic performance of this alloy,

and this point should be borne in mind in the discussion around weld defects in these specimens that occurs later in the paper.

Fatigue specimens were tested in tension-tension loading at $R = 0.1$ and had a width of 18 mm across the gauge length. Their surfaces were machined smooth to avoid initiation at shoulder marks, as the intrinsic performance of the welded material was required. Fatigue performance was assessed by testing at a single stress level that was applied to all specimens. An initial estimate of an appropriate stress was obtained from the S–N curve for the parent plate, where a stress of 216 MPa corresponded to a mean life of 10^6 cycles and 242 MPa to a life of about 2×10^5 cycles. Welded specimens were tested at 242 MPa, because previous work on this alloy [7] had indicated that the pseudo-bond defects were activated at higher levels of plastic strain and their effects are therefore more likely to be an influence at shorter fatigue lives. S–N data for welded specimens often exhibits a cross-over in performance ranking between 10^5 and 10^6 cycles and future work will consider the longer life performance of the welds. Fatigue life data for each weld, averaged from five specimens, are shown in Table 3.

The question that this paper seeks to answer, relates to determining an appropriate characterising parameter to relate input weld process parameters (tool rotational speed, feed rate, pitch) to the induced parameters of heat input and frictional power. If correlations can be found between these two energy parameters (heat input and frictional power) and the tensile strength and fatigue life of the welded specimens, then it should be possible to explain and predict weld performance using basic weld process parameters. Table 3 is not particularly illuminating in this respect, as the raw data does not show any clear trends. It is therefore necessary to calculate energy input and to relate heat and power input to the required performance parameters of tensile strength and fatigue life.

Fatigue life may be strongly influenced by the presence of residual stresses and extensive measurements of longitudinal and transverse residual stresses were made on sections 150 mm long cut from the middle of these welded plates. These measurements used synchrotron X-ray diffraction on beamline ID31 at the European Synchrotron Radiation Facility in Grenoble, France (experiment ME 992). These will not be covered in detail in this paper, but full experimental conditions and results are reported in Ref. [9].

2.1. Energy calculations

As noted in Fig. 1, key interactions between process parameters and weld mechanical and fatigue properties should be amenable to characterisation through energy input. Several workers have previously proposed equations to characterise welding energy during FSW, and process understanding of FSW is made more complicated by the unique self generation of heat that results from either friction between the weld tool and workpiece or from deformation heating associated with shearing within the workpiece [10]. In this work the energy input into the weld has been calculated using two routes; firstly using a heat input approach

Table 3
Fatigue life for each combination of process parameters

RPM	400	266	201	
Pitch (mm/rev)	0.21	0.32	0.42	
Feed[a] (mm/min)	85	85	85	
Fatigue life[b] (cycles)	21521	68798	50000	
RPM	635	423	318	254
Pitch (mm/rev)	0.21	0.32	0.42	0.51
Feed (mm/min)	135	135	135	135
Fatigue life (cycles)	74616	12746	14818	28624
RPM	870	617	436	348
Pitch (mm/rev)	0.21	0.30	0.42	0.53
Feed (mm/min)	185	185	185	185
Fatigue life (cycles)	32694	85897	16792	45021

[a] Tool feed rate during weld manufacture.
[b] Average of five tests for each welded plate.

due to Khandkar et al. [11] that is based on the tool torque and, secondly, a frictional power approach. The average heat input under the tool shoulder is given in Eq. (1):

$$Q_{in1} = \eta \frac{2\pi\omega \text{Torque}}{f} \tag{1}$$

where η is the efficiency of heat transfer into the weld (typically about 0.9), ω is the tool speed in rev/min and f is the feed rate in mm/min. Heat input has a strong correlation with details of the residual stress distribution in the welds [9] and, in particular, there is a linear correlation with the maximum value of the longitudinal residual stress and there is also an inverse linear correlation with the width of the HAZ. Fig. 5 demonstrates the

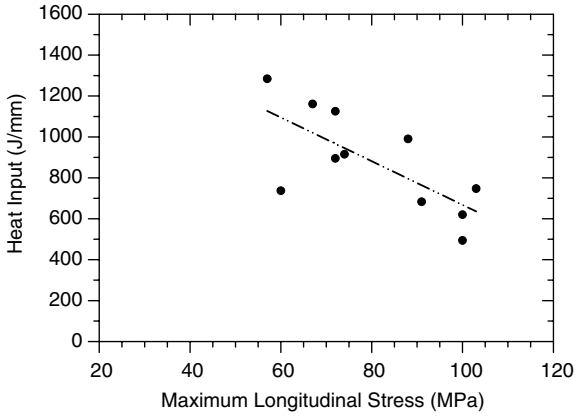

Fig. 5. Correlation between maximum longitudinal residual stress and heat input.

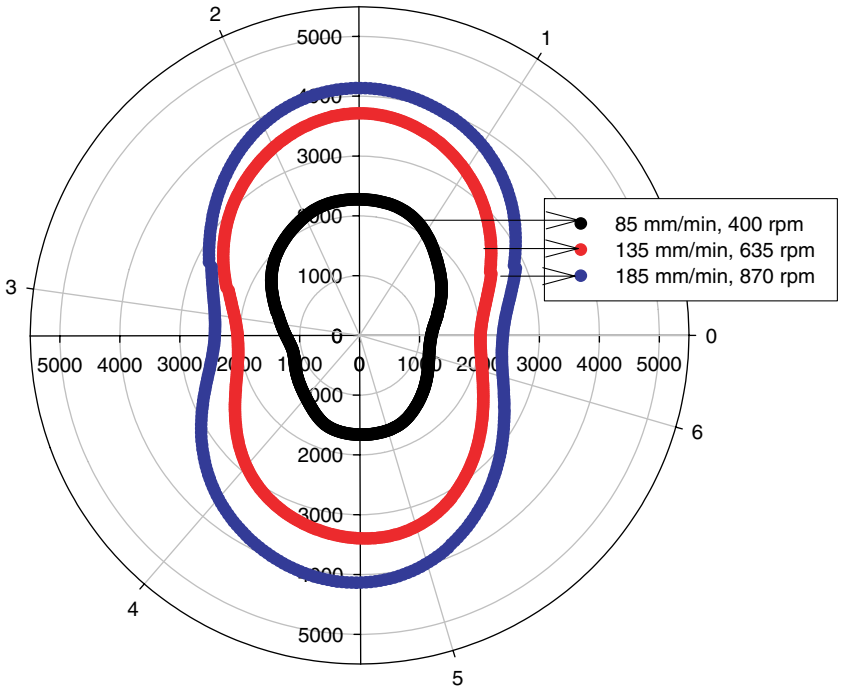

Fig. 6. Polar plots of resultant force during FS welding at three combinations of tool speed and feed giving a constant pitch of 0.2 mm/rev.

good linear correlation between heat input and maximum longitudinal residual stress. The polar plot of resultant force exerted on the tool is a useful graphical representation of heat input into the weld and the measured maximum value of resultant force also shows a good linear correlation with the maximum value of longitudinal residual stress. Fig. 6 shows polar plots of resultant force at a tool pitch of 0.2 mm/rev for three combinations of tool rotational speed and feed. The interest in polar force 'footprint' plots centers on their shape and rotation, which are believed to reflect aspects of the plastic flow around the tool.

The frictional power expression used in this work (Eq. (2)) is due to Frigaard and Midling [12] and uses an effective coefficient of friction defined by Santella et al. [13]

$$P_{in1} = \frac{4}{3}\pi\mu F_Z \omega r \tag{2}$$

where μ is an effective coefficient of friction under the tool shoulder, F_Z is the downwards force on the tool and r is the radius of the tool shoulder. Frictional power correlates well with tensile properties as is demonstrated in Fig. 7. Lower values of frictional power input provide higher tensile strengths, and this can be related to the necessity of establishing high enough temperatures to ensure adequate plasticisation of the alloy during the welding process; this in turn leads to a lower power requirement during welding. The relationship between average fatigue life (given in Table 3) and frictional power (calculated using Eq. (2)) is shown in Fig. 8 and

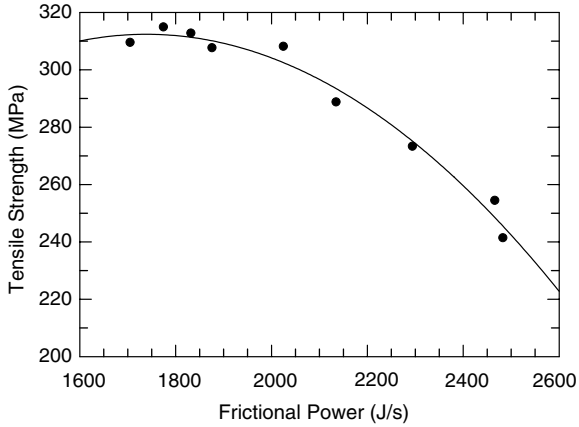

Fig. 7. Frictional power input versus tensile strength.

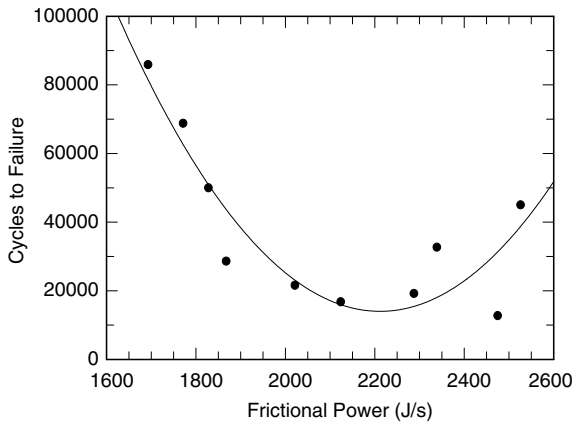

Fig. 8. Correlation between frictional power and fatigue life of welds at an applied tensile stress of 242 MPa.

again a good correlation exists between the process characteristic and the dynamic performance parameter. Lower frictional power (which, as noted above, occurs when temperatures during welding are high enough to give 'adequate' plasticisation for a good weld bond to be made) gives the highest observed fatigue lives at this value of applied stress, although fatigue life appears to be increasing again at the higher values of frictional power. Fig. 9 plots tensile strength against fatigue performance and it is interesting to note that the correlation between the static and dynamic performance indicators is not as good as might be expected from their individual correlations with frictional power. As will be discussed in the next section, this reflects the greater influence that the pseudo-bond defects have on fatigue crack paths, in particular the very detrimental effects of large planar facets on crack initiation. No correlation was found between the 0.2% proof strength and the fatigue life. As fatigue crack initiation is a yield-related phenomenon, this observation supports a conclusion that crack path effects are the primary cause of the relatively low ratios of tensile strength (expressed as

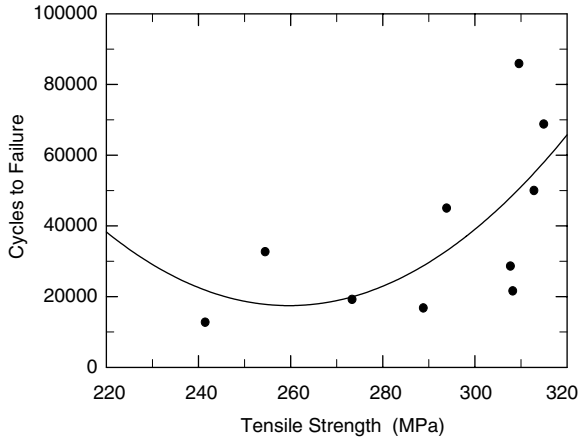

Fig. 9. Relationship between tensile strength and fatigue life measured under an applied tensile stress of 242 MPa.

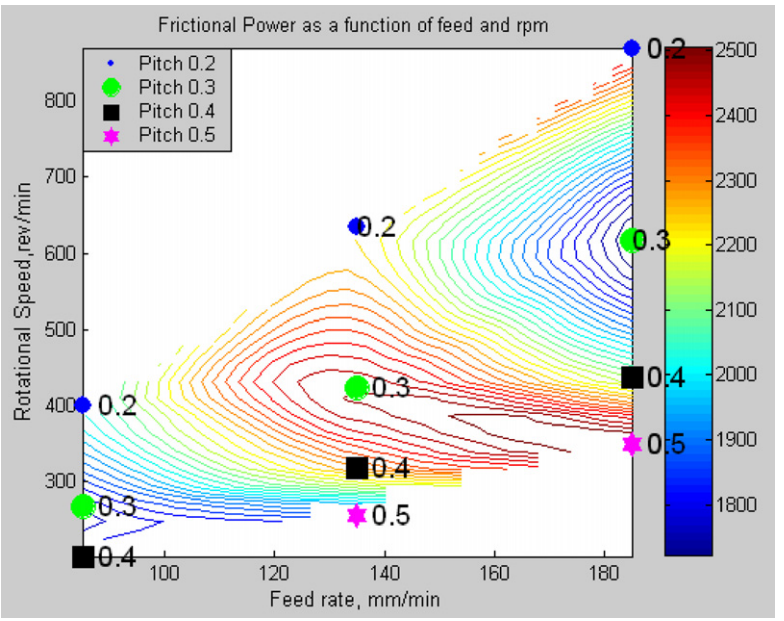

Fig. 10. Frictional power as a function of tool rotational speed and feed rate.

welded/parent plate values) observed in this alloy and that they also dominate fatigue crack initiation and growth.

Lower values of frictional power occur in two specific tool speed and feed regimes, as is shown in Fig. 10. The high speed and feed regime of low frictional power in Fig. 10 is centred around 600 rpm and 185 mm/min, while the low speed regime occurs below 300 rpm and 140 mm/min. Thus for this 5083-H321 aluminium alloy, one can predict the likely tool speed and feed regimes for this tool geometry that would lead to FS welds with a combination of high tensile strength and high values of low cycle fatigue life. Further work is required to examine this hypothesis at fatigue lives $>2\times10^6$ cycles.

3. Crack path effects

The relationships discussed so far have demonstrated linkages between: heat input, resultant force exerted on the tool by the plasticised metal, longitudinal residual stresses and width of the HAZ; and between frictional power input, tensile strength and fatigue life (at least at one particular value of applied tensile stress). It would generally be expected that there would be a relationship between weld defects and tensile strength [14], and therefore between defects, frictional power and the process parameters of tool speed and feed [15]. Welds in 5083-H321 contain significant pseudo-bond defects in the form of planar regions on the fracture surface and in the form of so-called onion-skin (OS) defects. Both of these defect types are defined below fractographically (Fig. 11), and have been observed previously to affect crack paths and fatigue strength [7,16]. Fig. 11 illustrates typical planar pseudo-bonds, sequences of onion-skin defects and also a high strength defect

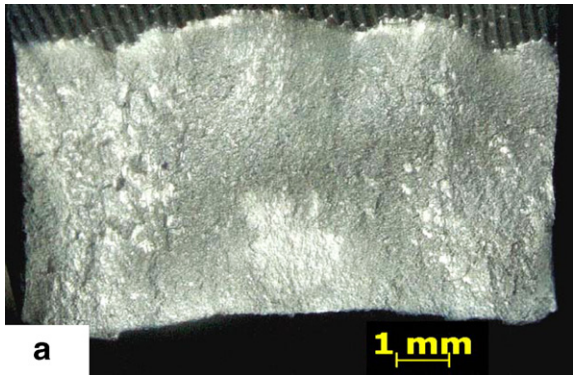

Fig. 11a. A defect-free tensile fracture surface: weld 3 with tensile strength = 313 MPa, tool feed rate = 85 mm/min, tool speed = 201 rpm and tool pitch = 0.42 mm/rev.

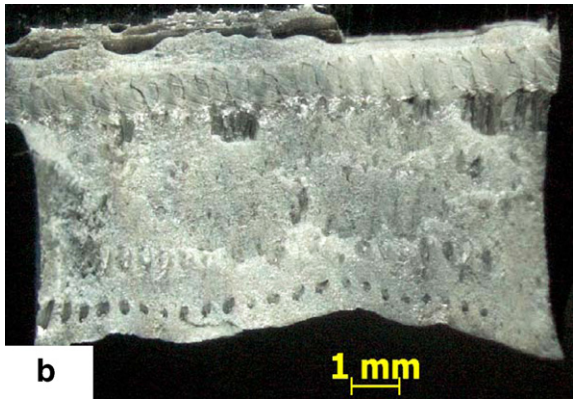

Fig. 11b. Onion-skin (OS) defects on a tensile fracture surface: weld 5 with tensile strength = 308 MPa, tool feed rate = 135 mm/min, tool speed = 254 rpm and tool pitch = 0.51 mm/rev.

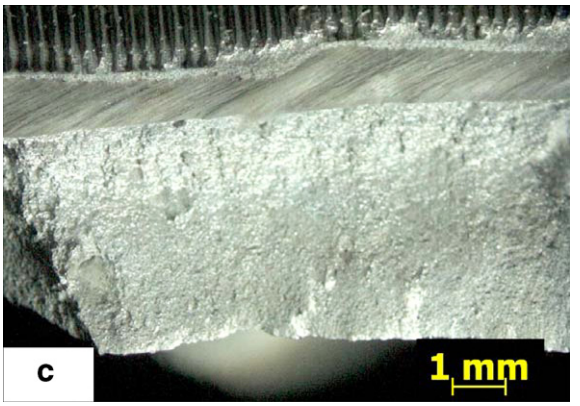

Fig. 11c. Planar facet (P) on a tensile fracture surface: weld 2 with tensile strength = 241 MPa, tool feed rate = 135 mm/min, tool speed = 423 rpm and tool pitch = 0.32 mm/rev.

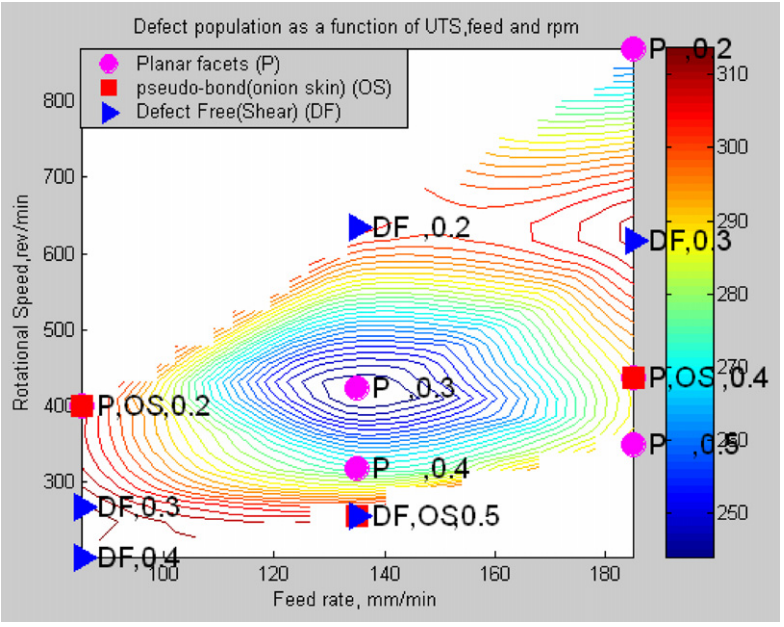

Fig. 12. Defect type and occurrence as a function of tensile strength and tool speed.

free fracture surface. These defects can be very extensive and their occurrence can be directly related to variability in tensile strength of the alloy, which ranges from 0.68 to 0.85 of the parent plate value (371 MPa). The 0.2% proof strength has a smaller percentage variation from 0.56 to 0.67 of the parent plate value (254 MPa). As the pseudo-bond defects are believed to have their origin in plastic flow effects in the TMAZ and to also be triggered by plastic deformation, their presence accounts for the greater variability observed in tensile strength. As noted earlier, these tensile and yield strength ratios for FS welds in this strain-hardened alloy are typical, and similar values have been reported by Peel [8].

Data presented in Ref. [8] indicated that tool feed and speed had an effect on the endurance limit in 5083-H321 alloy, and that finding is both confirmed and extended in the present work. Fig. 12 summarises the relationship between defects, tensile strength and tool speed and feed. As expected, the contour plot is the inverse of that seen in Fig. 10, and high tensile strengths correlate reasonably well with defect-free fracture surfaces.

There is insufficient data to draw firm conclusions, but there is an indication that OS defects occur in mid-range frictional power regimes, whilst planar facets occur in both medium and low power regimes. It is clear, however, that larger pseudo-bond defects on the fracture lead to lower tensile strength values and the planar facets are generally much larger in extent than the OS defects. Hence they tend to have a very detrimental effect on tensile strength while the OS defects are variable in influence.

3.1. Fatigue crack paths

The paper thus far has provided a brief overview of the systematic manner in which the present research programme has attempted to analyse the relationships amongst weld input parameters (tool speed and feed), material-dependent process parameters like energy input, and the output parameters of interest to weld and static structural performance, i.e. residual stress, tensile strength and defects. This information is a necessary precursor to understanding the fatigue behaviour of a strain-hardened alloy like 5083-H321, which is subject to extensive recrystallisation in the weld nugget during FSW and where the defects that occur during welding are likely to be triggered by plastic strain [7]. In general, welds made under different process conditions often show a cross-over in dynamic performance in going from the high stress-short life regime ($\sim 5 \times 10^4$ cycles) to

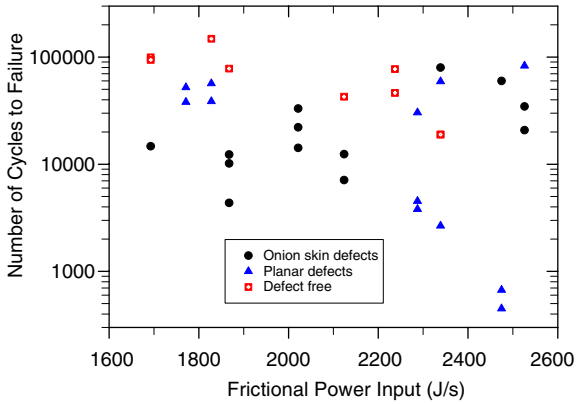

Fig. 13. Fatigue life as a function of defect type and power input.

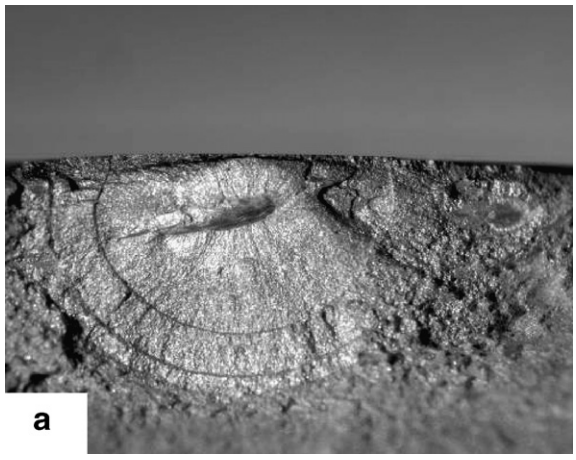

Fig. 14a. Typical fatigue crack initiation site in weld 2: tensile strength = 241 MPa, tool feed rate = 135 mm/min, tool speed = 423 rpm and tool pitch = 0.32 mm/rev and average fatigue life = 12746 cycles.

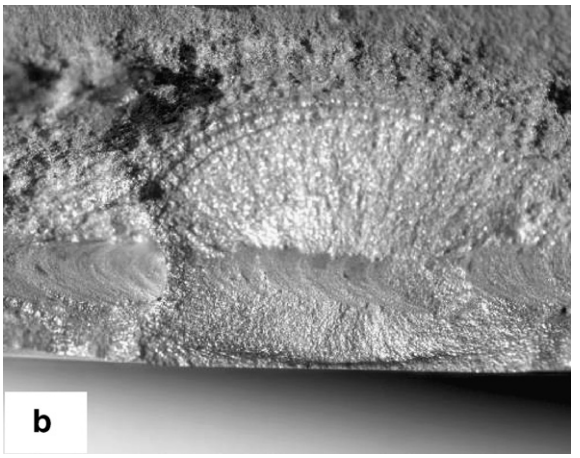

Fig. 14b. Typical fatigue crack initiation site in weld 7: tensile strength = 294 MPa, tool feed rate = 185 mm/min, tool speed = 348 rpm and tool pitch = 0.53 mm/rev and average fatigue life = 45021 cycles.

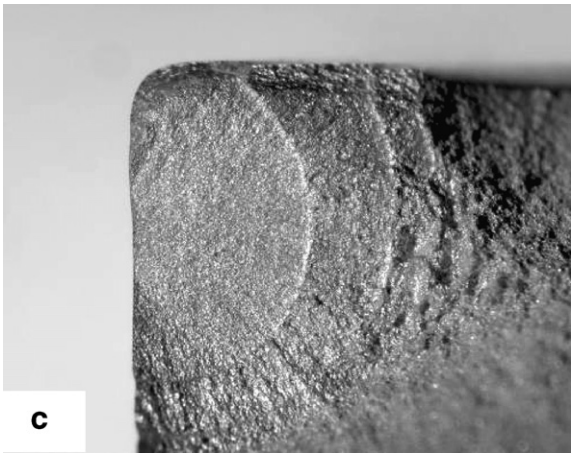

Fig. 14c. Typical fatigue crack initiation site in weld 10: tensile strength = 310 MPa, tool feed rate = 185 mm/min, tool speed = 617 rpm and tool pitch = 0.30 mm/rev and average fatigue life = 85897 cycles.

the low stress-long life regime ($>10^6$ cycles). This reflects their ability to reduce local strain concentrations through plastic flow and for the specific case of 5083-H321 alloy, the presence and triggering of pseudo-bond defects. To date, a single value of applied tensile fatigue stress has been considered which corresponds to a life of around 2×10^5 cycles in the parent plate, and lives between 300 and 1.5×10^5 cycles in the welded specimens. It has been shown that relationships exist among defect type, average fatigue life, average tensile strength and frictional power.

Fig. 13 presents the fatigue life data for all the individual specimens tested in this programme of work. Interestingly, in the relatively limited dataset available, the life of specimens containing onion-skin defects shows a slight increasing trend as frictional power increases, while those specimens containing planar defects show a bifurcation in behaviour as frictional power increases. These trends can be explained in terms of the relative sizes of the defects, and their extent across the weld, which reflect the underlying plastic flow processes in the TMAZ. These, in turn, reflect frictional power input and hence process parameters. Fatigue life is highly sensitive to influences on the crack initiation phase and to the existence of any easy growth routes in-plane with the fatigue crack. Whilst it could be argued that any influences on crack initiation would have a small effect in the low cycle fatigue regime, the fracture surfaces shown in Fig. 14 indicate that the pseudo-bond

defects in this alloy offer significantly enhanced crack initiation sites and are often associated with crack growth over several millimetres. It is clear that optimum fatigue life requires both defect-free welds and frictional power input below about 1900 J/s. Fig. 10 indicates that this requires particular combinations of tool speed and feed rate, while Fig. 12 indicates the occurrence of defects is governed by rotational speed of the tool and that for this tool geometry and alloy condition, rotational speeds of 615–635 rpm and <265 rpm offer the highest chance of defect-free welds. Future work will consider whether the polar force footprint diagrams can be interpreted to provide insights into why these particular tool speeds should produce appropriate plasticisation conditions in the TMAZ to minimise defect occurrence.

4. Conclusions

This work has demonstrated that there is significant potential to understand and model heat and power input during friction stir welding and to predict the likely tensile and fatigue performance resulting from particular combinations of tool feed rate and rotational speed. It has demonstrated that rotational speed governs defect occurrence in this 5083-H321 aluminium alloy and that there is a strong correlation between frictional power input, tensile strength and low cycle fatigue life. Part of this correlation arises from defect-induced crack path effects during fatigue crack growth. Values of peak longitudinal residual stress reflect the heat input during welding, as does the width of the HAZ (and hence the width of the residual stress peak). Future investigations of FSW using instrumented welding tools will allow a much less empirical approach to be developed to making welds with optimised sets of process parameters.

References

[1] Mishra RS, Ma ZY. Mater Sci Engng R 2005;50(1–2):1–78.
[2] Zhang HW, Zhang Z, Chen JT. J Mater Process Technol 2007;183(1):62–70.
[3] Attallaha MM, Salem HG. Mater Sci Engng A 2005;391:51–9.
[4] Okuyucu H, Kurt A, Arcaklioglu E. Mat Des 2007;28:79–84.
[5] Kim YG, Fujii H, Tsumura T, Komazaki T, Nakata K. Mat Lett 2006;60:3830–7.
[6] Hattingh DG, van Niekerk TI, Blignault C, Kruger G, James MN. IIW J Weld World 2004;48(1–2):50–8.
[7] James MN, Bradley GR, Lombard H, Hattingh DG. Fatigue Fract Engng Mater Struct 2005;28:245–56.
[8] Peel MJ. The Friction-Stir Welding of Disssimilar Aluminium Alloys, Ph.D Thesis, University of Manchester; 2005.
[9] Lombard H, Hattingh DG, Steuwer A, James MN. In: Proccedings of the 6th international symposium friction stir welding, Montreal, Canada, 10–12 October; 2006.
[10] Schneider J, Beshears R, Nunes Jr AC. Mater Sci Engng A 2006:297–304.
[11] Khandkar MZH, Khan JA, Reynolds AP. Sci Technol Weld Join 2003;8(3):165–74.
[12] Frigaard ØG, Midling OT. Met Mater Trans 2001;32A(5):1189–200.
[13] Santella M, Grant G, Arbegast W. In: Proceedings of the 4th international symposium friction stir welding, Utah, USA, 14–16 May; 2003.
[14] Liu HJ, Fujii H, Maedaa M, Nogi K. J Mater Proc Technol 2003;142:696.
[15] Chen H-B, Yan Y, Lin T, Chen S-B, Jiang C-Y, Zhao Y. Mater Sci Engng A 2006;433:64–9.
[16] James MN, Hattingh DG, Bradley GR. Int J Fatigue 2003;25:1389–98.